BULLETIN OF THE POLISH ACADEMY OF SCIENCES
TECHNICAL SCIENCES, Vol. 70(3), 2022, Article number: e141007
DOI: 10.24425/bpasts.2022.141007

Thermoelectric properties of bismuth-doped magnesium silicide obtained by the self-propagating high-temperature synthesis

Bartosz BUCHOLC [1], Kamil KASZYCA [1], Piotr ŚPIEWAK [2], Krzysztof MARS [3], Mirosław J. KRUSZEWSKI [2], Łukasz CIUPIŃSKI [2], Krystian KOWIORSKI [1], and Rafał ZYBAŁA [1,2]*

[1] Łukasiewicz Research Network – Institute of Microelectronics and Photonics, Aleja Lotników 32/46, 02-668 Warsaw, Poland
[2] Faculty of Materials Science and Engineering, Warsaw University of Technology, Wołoska 141, 02-507 Warsaw, Poland
[3] Faculty of Materials Science and Ceramic, AGH University of Science and Technology, Kraków, Al. Mickiewicza 30, 30-059, Poland

Abstract. Doping is one of the possible ways to significantly increase the thermoelectric properties of many different materials. It has been confirmed that by introducing bismuth atoms into Mg sites in the Mg_2Si compound, it is possible to increase career concentration and intensify the effect of phonon scattering, which results in remarkable enhancement in the figure of merit (ZT) value. Magnesium silicide has gained scientists' attention due to its nontoxicity, low density, and inexpensiveness. This paper reports on our latest attempt to employ ultrafast self-propagating high-temperature synthesis (SHS) followed by the spark plasma sintering (SPS) as a synthesis process of doped Mg_2Si. Materials with varied bismuth doping were fabricated and then thoroughly analyzed with the laser flash method (LFA), X-ray diffraction (XRD), scanning electron microscopy (SEM) with an integrated energy-dispersive spectrometer (EDS). For density measurement, the Archimedes method was used. The electrical conductivity was measured using a standard four-probe method. The Seebeck coefficient was calculated from measured Seebeck voltage in the sample subjected to a temperature gradient. The structural analyses showed the Mg_2Si phase as dominant and Bi_2Mg_3 located at grain boundaries. Bismuth doping enhanced ZT for every dopant concentration. ZT = 0.44 and ZT=0.38 were obtained for 3wt% and 2wt% at 770 K, respectively.

Key words: thermoelectric materials; magnesium silicide; bismuth doping; SHS; spark plasma sintering.

1. INTRODUCTION

As one of many consequences of global climate change, great attention has been paid to enhancing the energy efficiency of industrial power plants and all other types of devices and installations using or generating energy. Thermoelectric generators (TEG), composed of thermoelectric materials with *n*-type and *p*-type conduction types, might be a solution when commonly used for efficient waste heat recovery. They facilitate the conversion of temperature gradient into electricity by the Seebeck effect. So far, several obstacles have prevented their widespread use, such as high production costs, the toxicity of processing byproducts, fabrication scalability challenges, and relatively low energy conversion efficiency. The last one is in positive correlation with the so-called dimensionless figure of merit ZT, which can be written as $ZT = \alpha^2 \cdot \sigma \cdot T \cdot \lambda^{-1}$, where α is the Seebeck coefficient, T is the temperature σ and λ stands for the electrical and thermal conductivity, respectively [1]. Among many different approaches to improving the aforementioned parameter, one can indicate alloying [2, 3], doping [4, 5], nanostructuring [6–8], nanocomposites fabrication [9, 10], or obtaining them in the form of thin films and superlattices [11–13]. The purpose of those treatments is usually to increase the power factor, which is the product of $\alpha^2 \cdot \sigma$, or reduce thermal conductivity λ. Attempts were made to combine the effects of both these factors.

Compared to other popular thermoelectric materials, Mg_2Si-based exhibit a unique combination of properties. Apart from the promising thermoelectric performance [14], low density [15], nontoxicity of its processing byproducts, and relatively low price of its primary constituents should be pointed out. To enable the use of Mg_2Si-based materials in practical applications, it would be advisable to produce equally efficient materials, with both types of conduction *p* and *n*, by an easily scalable method. Since the first investigations of its thermoelectric properties in the 1960s [16], many dopants and manufacturing techniques have been tested. Aside from the conventional ceramic method, some novel advanced procedures have been employed. Berthebaud and Gascoin used the microwaved assisted fast synthesis to fabricate *n* and *p*-doped Mg_2Si [17]. For the *n*-type material, the highest value of ZT was achieved for antimony and tin doping (0.7 at 770 K), and in the case of *p*-type addition of silver resulted in ZT of 0.35 at 770 K. Nakagawa *et al.* synthesized Mg_2Si by the liquid encapsulated vertical gradient freezing method [18]. The vertical Bridgman method was used for bulk crystal growth by Yoshinaga *et al.* to

*e-mail: Rafal.Zybala@pw.edu.pl

Manuscript submitted 2022-02-17, revised 2022-02-179, initially accepted for publication 2023-03-03, published in June 2022.

achieve a power factor of $7.8 \cdot 10^{-6}$ $Wcm^{-1}K^{-2}$ at 373 K [19]. Fu *et al*. suggested the vacuum plasma thermal spray (VPS) as a potential deposition technique for thermoelectric materials [20]. They obtained samples of Mg_2Si with maximum ZT = 0.16 at 700 K.

In addition to Ag, Sb and Sn doping also reports of Cu [21], Li [22], Al [21], Co [17] and Bi [14,15,21–24] should be noted. Especially the last one has gained a lot of attention since its first investigation in 2005 by Tani and Kido [14], who fabricated $Mg_2Si_{0.98}Bi_{0.02}$ exhibiting ZT = 0.86 at 862 K. Since then, attempts have been made to increase that value, and synthesize such material with various methods. Choi *et al.* utilized the vacuum melting method followed by Spark Plasma Sintering (SPS) [23]. The same method for consolidation was used by Nieroda *et al.* to densify material obtained by direct synthesis [15]. In their work, they annealed bulk samples for seven days to improve homogeneity resulting in ZT = 0.55 at 720 K. Li *et al*. in their paper presented Bi-doped Mg_2Si with one of the highest values of ZT equal to 0.98 at 883 K [25]. The preparation route included high-pressure synthesis and SPS. Each processing route mentioned is energy and time-consuming or very difficult to scale. To ensure the economic viability of the thermoelectric materials manufacturing process, it is necessary to use adaptable techniques for large-scale production, such as fast self-propagating high-temperature synthesis (SHS) [26]. This technique was successfully employed by Zhang *et al*. for the synthesis of Sb doped Mg_2Si in [27] and Cu_2Se in [28]. To our knowledge, there was no published paper on the utilization of this method for Bi-doped Mg_2Si.

Bearing that in mind, in this work, we report on our latest attempt to employ fast synthesis for bismuth-doped magnesium silicide followed by spark plasma sintering. Materials obtained with different dopant content were scrutinized. The Seebeck coefficient, and electrical and thermal conductivity, were measured in the temperature range of 300-800 K. The measurements conducted allowed us to determine dopant content that resulted in the highest ZT value. Moreover, the microstructural investigations using X-ray diffraction (XRD) and scanning electron microscope (SEM) were carried out to evaluate its correlation with the thermoelectrical properties.

2. MATERIALS AND METHODS

2.1. Materials synthesis

Samples for further investigation were prepared from high purity powders of Mg (99.8%, $-20+100$ mesh), Si (99.99%, $-100+100$ mesh) and Bi (99.999%, $-100+100$ mesh). After being weighed in the stoichiometric ratio of $Mg_2Si_{1-x}Bi_x$ ($x = 0, 0.01, 0.02, 0.03$) for MG0, MG1, MG2, MG3 samples, respectively, powders were then homogenized in a mechanical mortar grinder. Homogenization was followed by the first stage of the synthesis, which was the self-propagating reaction held in a graphite die at 550 °C. The reaction was triggered by heating of the die, which was stopped when the temperature increase caused by the exothermic synthesis reaction occurred. Subsequently, the reaction product was ground into powder and poured into the graphite die for the second stage of the synthesis process, the purpose of which was to homogenize the material. That was achieved by annealing the powder at 500 °C for 2 min. The heating and cooling rates for both stages were 100 °C min^{-1}. Later, the material was ground into a fine powder and subjected to a consolidation process conducted by the spark plasma sintering technique (SPS). The fabrication process is depicted in Fig. 1. Sintering parameters for all the bulk samples obtained are given in Table 1.

Table 1

Parameters of the spark plasma sintering processes

Sintering parameter	$Mg_2Si_{1-x}Bi_x$
Maximum pressure applied [MPa]	50
Temperature [°]	750
Time [min]	15

2.2. Materials characterization

X-ray diffraction (XRD) analyses were performed to investigate the influence of the consecutive stages of the synthesis processes on the materials' microstructural properties. The phase compositions were identified with an X-ray diffractometer (Bruker D8 Advance, Cu Kα radiation). A scanning electron

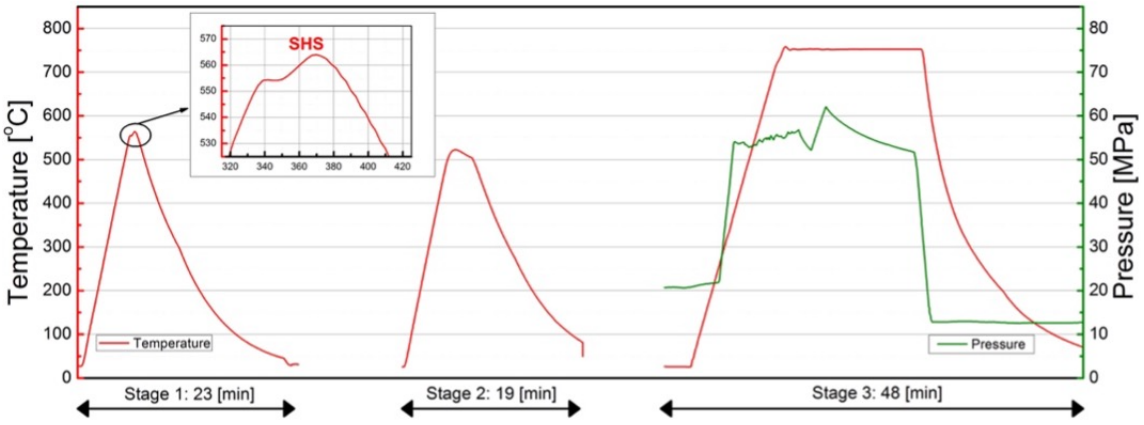

Fig. 1. Synthesis and sintering parameters of the fabricated materials

microscope (SEM) equipped with an energy dispersive spectrometer (EDS) was used for microstructure observations, elemental mapping, and point analysis of the samples embedded in epoxy resin and later polished with a diamond paste (CrossBean Auriga, Carl Zeiss). The electrical conductivity σ, and the Seebeck coefficient α of all the samples were measured using a specially designed apparatus (SeebTest, PESS). A thorough description of this method can be found in the authors' previous work [7]. The thermal diffusivity D of the materials was measured using the laser flash method (LFA 457, Netzsch).

3. RESULTS

3.1. X-ray diffraction (XRD)

Figure 2 shows selected diffraction patterns for MG1 after each subsequent fabricating step. The diffraction peaks of Si and Mg gradually become increasingly less intense, and finally, the reflection of Si disappears completely - this phenomenon occurs in all MG1-MG3 samples. Mg_2Si phase was significantly dominant on every fabrication step. After the sintering process for all Bi-doped samples, X-ray diffraction analysis indicate the presence of impurities in the form of Bi_2Mg_3 and Mg phases. In the case of undoped Mg_2Si after the SPS process, the diffraction peaks of Si and Mg were detected.

With the whole powder pattern fitting (WPPF) method, the content of each phase component was estimated for MG3 after synthesis steps and sintering. The results are given in Table 2.

Table 2
MG3 phase composition obtained with the WPPF method

Stage of synthesis	Phase composition			
	Mg_2Si	Bi_2Mg_3	Mg	Si
1st (SHS)	84.10	3.63	7.85	4.42
2nd	91.80	4.28	2.14	1.78
3rd (SPS)	94.99	4.15	1.78	0.00

3.2. SEM microstructural observation

The SEM observations were made on the metallographic section and a fractured sample. For selected areas and points EDS was utilized to investigate the chemical composition of materials in analyzed images. Figure 3 shows selected SEM images with corresponding elemental mapping for Mg, Si, and Bi for MG3. Both Mg and Si seem to be uniformly distributed in the analyzed area, whereas the central region has a visibly lower content of Bi. Sintered samples show almost no porosity.

Figure 4 depicts an SEM image of the fractured MG3 sample. Between the grains of the Mg_2Si, a white phase exhibiting significant Bi content can be seen – Bi_2Mg_3, which was confirmed with EDS and XRD analyses.

3.3. Electrical properties

The Seebeck coefficient α measured in the temperature range of 300–800 K for all samples, is presented in Fig. 5. All investigated materials exhibit negative signs of the Seebeck coefficient within the entire range. The sample of Mg_2Si with no bismuth addition shows higher values in comparison to other samples, and it rises from –300 μVK^{-1} at 350 K to over –400 μVK^{-1} at 425 K and then monotonically falls below –200 μVK^{-1} at maximum temperature. For samples of MG1 and MG3 a similar tendency is observed. Both slightly drop at 350 K and 625–675 K, but apart from that, both monotonically increase from 100 μVK^{-1} to 154 μVK^{-1} and 93 μVK^{-1} to 146 μVK^{-1}, respectively. Among doped Mg_2Si samples, the highest values of the Seebeck coefficient for all measured points exhibits MG2, and it is between 10–30 μVK^{-1} higher than for MG1 sample, achieving its maximum of 174 μVK^{-1} at 770 K. Figure 6 depicts the temperature-dependent electrical conductivity, σ, in the range of 300–800 K. Between 300–550 K MG0 sample shows very low and almost constant electrical conductivity, which starts increasing above 550 K and reaches $4.3 \cdot 10^1$ Sm^{-1} at 770 K. It has the lowest values in the entire range compared to other samples.

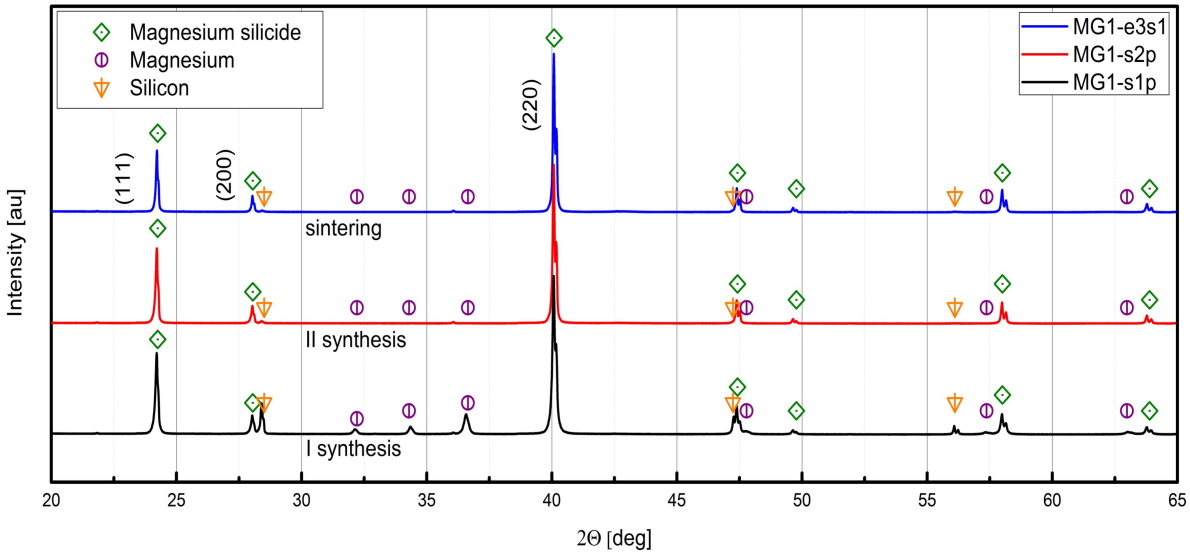

Fig. 2. Diffraction patterns for MG1 obtained at subsequent fabrication steps

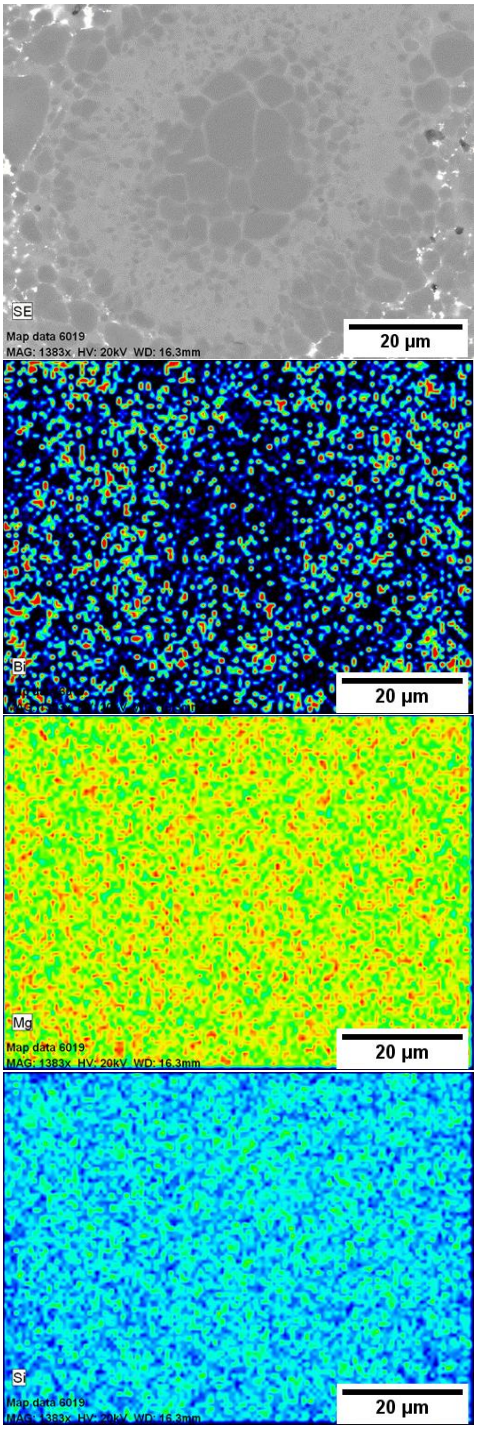

Fig. 3. Selected SEM image with corresponding element maps of Bi, Mg and Si for MG3 sample

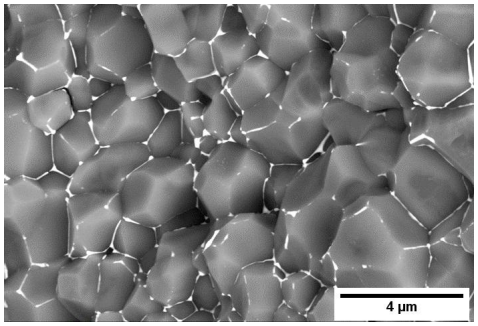

Fig. 4. SEM image of the fractured MG3 sample

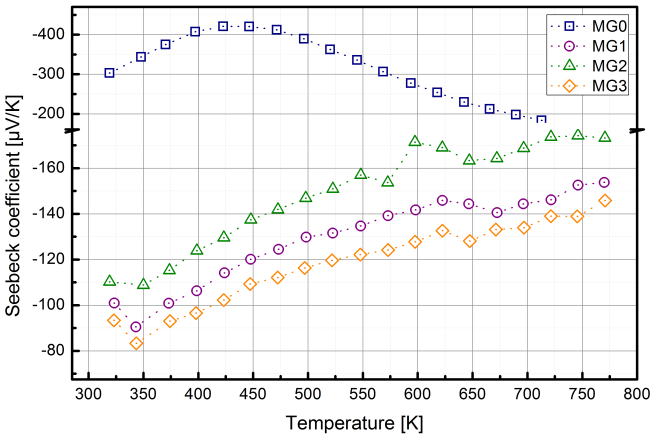

Fig. 5. Temperature dependency of Seebeck coefficient

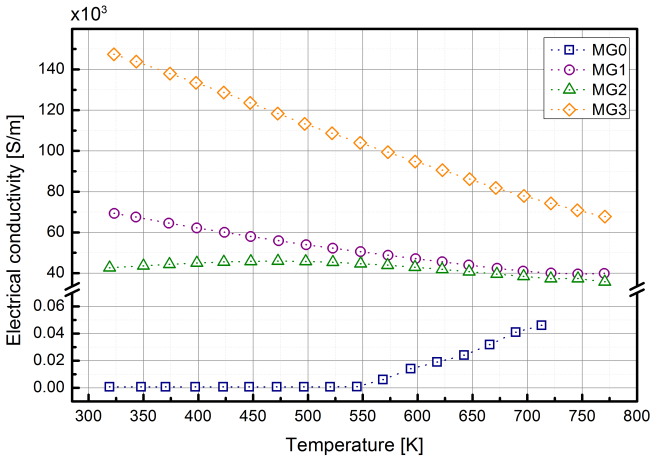

Fig. 6. Temperature dependency of electrical conductivity

On the other hand, the highest electrical conductivity has the MG3 sample (with the highest bismuth doping content of 3wt%). It exhibits almost $1.5 \cdot 10^5$ Sm^{-1} at 350 K and subsequently linearly decreases to 6.8×10^4 Sm^{-1}. The electrical conductivity of MG1 decreases in the entire temperature range from $7.0 \cdot 10^4$ Sm^{-1} to $4.0 \cdot 10^4$ Sm^{-1}. On the contrary, values for the MG2 sample exhibit insignificant fluctuations between $3.8-4.4 \cdot 10^4$ Sm^{-1}.

3.4. Thermal properties

The laser flash method was used for estimation of the thermal diffusivity, D, in turn, which is necessary for the thermal conductivity calculation according to the equation $\lambda = D \cdot C_p \cdot \rho$, where ρ is the density of the material (measured by the Archimedes method in water), and the C_p is the specific heat capacity (assumed as well-known material property and obtained from literature).

The results of temperature-dependent thermal conductivity λ, obtained for all samples are presented in Fig. 7. In all the cases, the thermal conductivity decreases over the measured temperature range. MG0 sample was characterized by heat conductivity in a range of 2.5 $Wm^{-1}K^{-1}$ to 1 $Wm^{-1}K^{-1}$. The highest thermal conductivity of 6.6 $Wm^{-1}K^{-1}$, which drops to 3.5 $Wm^{-1}K^{-1}$, has the MG3 doped sample. The MG1 sample exhibits a similar thermal conductivity enhancement at a lower temperature; however, it decreases below 3 $Wm^{-1}K^{-1}$ at 770 K. Material with medium dopant content MG2 exhibits the thermal conductivity of 5.5 $Wm^{-1}K^{-1}$ which later drops to the level of MG1 sample.

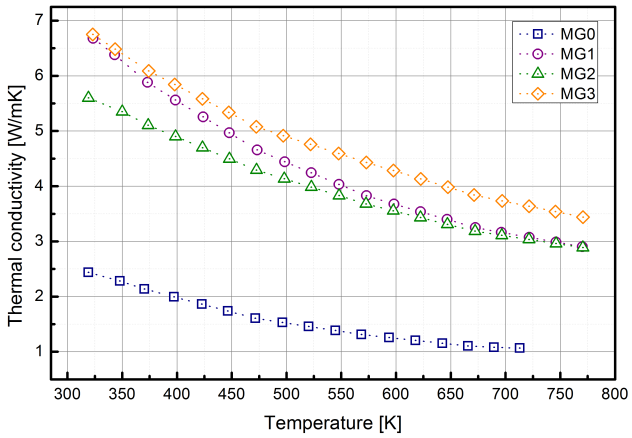

Fig. 7. Temperature dependency of thermal conductivity

3.5. ZT parameter

Calculated values of the figure of merit are presented in Fig. 8. Its value for MG0 in the range of 320–550 K is very close to 0 and then slightly increases to 0.0015 at the temperature of 700 K. ZT parameter for doped samples increased significantly across the temperature range. The most significant change is reported for MG2. It rises from 0.09 at low temperature to 0.38 at 770 K, but the most highly doped material reaches the highest values at all measuring points. At 770 K, the MG3 sample exhibits ZT = 0.44.

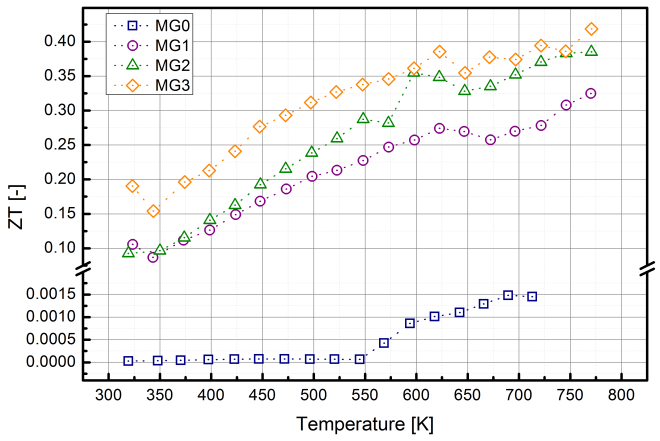

Fig. 8. Temperature dependency of the figure of merit ZT

4. DISCUSSION

XRD analysis presented in Table 2 shows that every synthesis step led to an increase in the content of Mg_2Si and a significant decrease in Si and Mg. The amount of Bi_2Mg_3 rises after annealing from 3.63% to 4.28% and then slightly diminishes to 4.15% after sintering. The changes in chemical composition occur not only during the first and the second steps of synthesis but also during the sintering process – the residuals of substrates are reacting with Si to create the Mg_2Si phase.

Figure 3 shows the non-porous, homogenous structure of Mg_2Si with the Bi_2Mg_3 phase at grain boundaries, which enhances the thermoelectric properties of synthesized material according to the phenomena described later in the discussion. There are areas with lower Bi_2Mg_3 phase concertation, but they can be observed only in the regions of large Mg_2Si grains. Figure 4 presents the magnified structure of obtained material, where Mg phases (Bi_2Mg_3 and pure Mg) are visible.

All the Bi-doped samples exhibit significantly higher electrical conductivity than the non-doped ones. In general, it is consistent with other works [14, 15, 23]. Firstly, this effect is due to the Bi atoms acting as donors when substituting Mg sites, causing the increase in the carrier concentration. Secondly, as proposed by Choi *et al.* [23], the presence of the Bi_2Mg_3 phase at grain boundaries might provide new transport paths for charge carriers. The microstructure observation showed that indeed the magnesium bismuth compound exists in the form of a percolating structure (see Fig. 4) throughout the entire material volume, which seems to be an important factor enhancing the electrical conductivity. MG1 and MG3 samples exhibit near-metallic electrical conductivity, decreasing with the increase of the temperature over the entire measuring range. That is associated with increased electron scattering leading to a reduction in the charge carrier mobility. As opposed to other works [14, 15], there was no direct composition-electrical conductivity dependence at low temperatures. The MG2 sample shows lower conductivity than the MG1. Furthermore, it exhibits an increase in the range of 325-525 K, which is more characteristic of the degenerate semiconductor than metallic materials. Above that temperature, the electrical conductivity falls slightly and reaches the values close to that measured for MG1 material. Clearly, also MG0 (non-doped Mg_2Si) shows semiconductor properties as its electrical conductivity rises above 550 K. This is consistent with other works [14, 29].

The Seebeck coefficient values for all the samples have negative signs across the whole temperature range. That indicates *n*-type behavior. Bismuth doping caused a significant reduction in the absolute value of the Seebeck coefficient with respect to the undoped Mg_2Si, especially at lower temperatures. The absolute value of the Seebeck coefficient of all the doped samples increases with the temperature rise. In general, that is in agreement with the works of other researchers [14, 15, 23, 29] and it is due to the increase in carrier concentration, but in this case, same as for the electrical conductivity, there is no visible composition dependence. The highest absolute value is achieved for the MG2 sample and the lowest for the MG3 sample. The MG1 sample has middling values across the temperature range.

The thermal conductivity measurements depicted in Fig. 7 show that bismuth doping enhances the heat transport properties. Values of the thermal conductivity for non-doped material (2.3 $Wm^{-1}K^{-1}$ at 350 K and 1.0 at 720 K) are much lower than reported by Tani and Kido (9 $Wm^{-1}K^{-1}$ at 350 K and over 4.0 at 720 K) [14] and Choi *et al.* (7 $Wm^{-1}K^{-1}$ at 300 K and around 3.5 at 750 K) for Mg_2Si also sintered with SPS method [23]. However, the values obtained for MG2 are close to those reported by Farahi *et al.* in 2014, especially at the higher temperature, who used the hot pressing technique to densify the material synthesized for 3.5 days and then annealed for another five days [30]. The fact that the thermal conductivity of Mg_2Si with no Bi addition does not increase with the increase of electrical conductivity above 550 K suggests a negligible influence of the electronic component of thermal conductivity.

The figure of merit for all samples rises as the temperature increases, mainly due to the rise of the Seebeck coefficient and decrease in the thermal conductivity. The highest ZT value for MG3 and MG2 samples were 0.44 and 0.38 at 770 K, respectively. Nieroda *et al*. for the same amount of bismuth dopant achieved ZT below 0.25 at 730 K after seven days of homogenization annealing at 1023 K followed by SPS [15]. Our result obtained for MG2 at 770 K doping is about 11% higher than that obtained by Fiameni *et al*., who fabricated this material using a method called mechanical alloying, i.e. long-lasting ball milling [31]. However, it is a significantly lower value than that reported by Kido and Tani for $Mg_2Si_{0.98}Bi_{0.02}$. Their investigations resulted in $ZT = 0.77$ at 770 K.

5. CONCLUSIONS

In this work, we successfully fabricated $Mg_2Si_{1-x}Bi_x$ ($x = 0$, 0.01, 0.02, 0.03) via ultra-fast self-propagating high-temperature synthesis (SHS) followed by spark plasma sintering (SPS). All bulk samples were thoroughly investigated to evaluate their microstructural and thermoelectric properties. The results of X-ray diffraction (XRD), observations done with the scanning electron microscope (SEM), measurements of the electrical conductivity and the Seebeck coefficient, as well as the thermal conductivity calculated from density, specific heat capacity, and the thermal diffusivity obtained with the laser flash method (LFA) were presented. Bismuth doping strongly affected all properties. A significant increase in the electrical and thermal conductivity was noted. However, Bi atoms caused a substantial reduction in the absolute value of the Seebeck coefficient with respect to nondoped Mg_2Si, especially at a lower temperature. All sintered Bi-doped samples X-ray diffraction analyses indicate a presence of impurities in the form of Bi_2Mg_3 and Mg phases. In the case of undoped Mg_2Si after the SPS process, the diffraction peaks of Si and Mg were detected. The highest value of $ZT = 0.44$ at 770 K was achieved for 3wt% Bi doping. What is remarkable about that result, compared to other works, is that the whole fabrication process was very rapid with no long-lasting annealing process. Although we confirm that the SHS might be considered a potential economically viable method for bismuth-doped Mg_2Si production, investigations towards enhancing its thermoelectric performance should be conducted in the future.

ACKNOWLEDGEMENTS

The presented research was supported by National Centre for Research and Development (NCBR, Poland) within a framework of the project entitled “Thermoelectric Transport Properties in Si-based and Ge-based Nanostructured Bulk Materials” (project no. PL-TW/IV/19/2016). This scientific work was partially financed by the National Science Centre (NCN, Poland) projects no.: 2016/23/D/ST8/02686 and 2017/27/N/ST8/01797.

REFERENCES

[1] R. Venkatasubramanian, E. Siivola, T. Colpitts, and B. O’Quinn, “Thin-film thermoelectric devices with high room-temperature figures of merit”, *Nature*, vol. 413, no. 6856, pp. 597–602, Oct. 2001, doi: 10.1038/35098012.

[2] G.S. Nolas, M. Kaeser, R.T. Littleton, and T.M. Tritt, “High figure of merit in partially filled ytterbium skutterudite materials”, *Appl. Phys. Lett.*, vol. 77, no. 12, p. 1855, 2000, doi: 10.1063/1.1311597.

[3] Y. Wang *et al.*, “Enhanced thermoelectric perfromance in cubic form of SnSe stabilized through enformatingly alloying $AgSbTe_2$”, *Acta Mater.*, vol. 227, p. 117681, Apr. 2022, doi: 10.1016/j.actamat.2022.117681.

[4] Y. Pei, X. Shi, A. LaLonde, H. Wang, L. Chen, and G.J. Snyder, “Convergence of electronic bands for high performance bulk thermoelectrics”, *Nature*, vol. 473, no. 7345, pp. 66–69, May 2011, doi: 10.1038/nature09996.

[5] R. Biswas, S. Vitta, and T. Dasgupta, “Influence of zinc content and grain size on enhanced thermoelectric performance of optimally doped ZnSb”, *Mater. Res. Bull.*, vol. 149, p. 111702, May 2022, doi: 10.1016/j.materresbull.2021.111702.

[6] J. R. Sootsman, D. Y. Chung, and M. G. Kanatzidis, “New and Old Concepts in Thermoelectric Materials”, *Angew. Chem. Int. Ed.*, vol. 48, no. 46, pp. 8616–8639, Nov. 2009, doi: 10.1002/anie.200900598.

[7] R. Zybała *et al.*, “Characterization of nanostructured bulk cobalt triantimonide doped with tellurium and indium prepared by pulse plasma in liquid method”, *Bull. Pol. Acad. Sci. Tech. Sci.*, vol. 68, no. 1, pp. 125–134, 2020, doi: 10.24425/BPASTS.2020.131835.

[8] G. Gabka *et al.*, “Facile Gram-Scale Synthesis of the First n-Type $CuFeS_2$ Nanocrystals for Thermoelectric Applications”, *Eur. J. Inorg. Chem.*, vol. 2017, no. 25, pp. 3150–3153, Jul. 2017, doi: 10.1002/ejic.201700611.

[9] K. Biswas *et al.*, “High-performance bulk thermoelectrics with all-scale hierarchical architectures”, *Nature*, vol. 489, no. 7416, pp. 414–418, Sep. 2012, doi: 10.1038/nature11439.

[10] F. Dąbrowski *et al.*, “Microstructure and thermoelectric properites od doped FeSi2 with addition of B4C nanoparticles”, *Arch. Metall. Mater.*, vol. 66, no. 4, pp. 1157–1162, 2021, doi: 10.24425/AMM.2021.136436.

[11] G. Chen, M. S. Dresselhaus, G. Dresselhaus, J.-P. Fleurial, and T. Caillat, “Recent developments in thermoelectric materials”, *Int. Mater. Rev.*, vol. 48, no. 1, pp. 45–66, Feb. 2003, doi: 10.1179/095066003225010182.

[12] R. Hu, Z. Zhou, C. Sheng, S. Han, H. Yuan, and H. Liu, "Ultralow lattice thermal conductivity and high thermoelectric performance of the WS2/WTe2 van der Waals superlattice", *Phys. Lett. A*, vol. 430, p. 127986, Apr. 2022, doi: 10.1016/j.physleta.2022.127986.

[13] R. Zybała *et al.*, "Synthesis and Characterization of Antimony Telluride for Thermoelectric and Optoelectronic Applications", *Arch. Metall. Mater.*, vol. 62, no. 2, pp. 1067–1070, Jun. 2017, doi: 10.1515/amm-2017-0155.

[14] J. Tani and H. Kido, "Thermoelectric properties of Bi-doped Mg_2Si semiconductors", *Phys. B Condens. Matter*, vol. 364, no. 1–4, pp. 218–224, Jul. 2005, doi: 10.1016/j.physb.2005.04.017.

[15] P. Nieroda, J. Leszczynski, and A. Kolezynski, "Bismuth doped Mg 2 Si with improved homogeneity: Synthesis, characterization and optimization of thermoelectric properties", *J. Phys. Chem. Solids*, vol. 103, pp. 147–159, Apr. 2017, doi: 10.1016/j.jpcs.2016.11.027.

[16] R.J. LaBotz, D.R. Mason, and D.F. O'Kane, "The Thermoelectric Properties of Mixed Crystals of $Mg_2Ge_xSi_{1-x}$", *J. Electrochem. Soc.*, vol. 110, no. 2, p. 127, 1963, doi: 10.1149/1.2425689.

[17] D. Berthebaud and F. Gascoin, "Microwaved assisted fast synthesis of n and p-doped Mg_2Si", *J. Solid State Chem.*, vol. 202, pp. 61–64, Jun. 2013, doi: 10.1016/j.jssc.2013.03.014.

[18] R. Nakagawa, H. Katsumata, S. Hashimoto, and S. Sakuragi, "Synthesis and crystal growth of Mg_2Si by the liquid encapsulated vertical gradient freezing method", *Jpn. J. Appl. Phys.*, vol. 54, no. 8, p. 085503, Jul. 2015, doi: 10.7567/jjap.54.085503.

[19] M. Yoshinaga, T. Iida, M. Noda, T. Endo, and Y. Takanashi, "Bulk crystal growth of Mg_2Si by the vertical Bridgman method", *Thin Solid Films*, vol. 461, no. 1, pp. 86–89, Aug. 2004, doi: 10.1016/j.tsf.2004.02.072.

[20] G. Fu, L. Zuo, J. Longtin, C. Nie, and R. Gambino, "Thermoelectric properties of magnesium silicide fabricated using vacuum plasma thermal spray", *J. Appl. Phys.*, vol. 114, no. 14, p. 144905, Oct. 2013, doi: 10.1063/1.4825045.

[21] T. Sakamoto *et al.*, "Thermoelectric Characteristics of a Commercialized Mg_2Si Source Doped with Al, Bi, Ag, and Cu", *J. Electron. Mater.*, vol. 39, no. 9, pp. 1708–1713, Sep. 2010, doi: 10.1007/s11664-010-1155-y.

[22] A. Kolezynski, P. Nieroda, and K. T. Wojciechowski, "Li doped Mg_2Si p-type thermoelectric material: Theoretical and experimental study", *Comput. Mater. Sci.*, vol. 100, pp. 84–88, Apr. 2015, doi: 10.1016/j.commatsci.2014.11.015.

[23] S.-M. Choi, K.-H. Kim, I.-H. Kim, S.-U. Kim, and W.-S. Seo, "Thermoelectric properties of the Bi-doped Mg_2Si system", *Curr. Appl. Phys.*, vol. 11, no. 3, pp. S388–S391, May 2011, doi: 10.1016/j.cap.2011.01.031.

[24] X. Cheng, N. Farahi, and H. Kleinke, "Mg_2Si-Based Materials for the Thermoelectric Energy Conversion", *JOM*, vol. 68, no. 10, pp. 2680–2687, Oct. 2016, doi: 10.1007/s11837-016-2060-5.

[25] J. Li *et al.*, "Enhanced thermoelectric performance of bismuth-doped magnesium silicide synthesized under high pressure", *J. Mater. Sci.*, vol. 53, no. 12, pp. 9091–9098, Jun. 2018, doi: 10.1007/s10853-018-2185-8.

[26] M.J. Kruszewski, Ł. Ciupiński, and R. Zybała, "Review of rapid fabrication methods of skutterudite materials", *Mater. Today Proc.*, vol. 44, pp. 3475–3482, 2021, doi: 10.1016/ j.matpr.2020.05.808.

[27] Q. Zhang *et al.*, "Phase Segregation and Superior Thermoelectric Properties of $Mg_2Si_{1-x}Sb_x$ (0?x?0.025) Prepared by Ultrafast Self-Propagating High-Temperature Synthesis", *ACS Appl. Mater. Interfaces*, vol. 8, no. 5, pp. 3268–3276, Feb. 2016, doi: 10.1021/acsami.5b11063.

[28] X. Su *et al.*, "Self-propagating high-temperature synthesis for compound thermoelectrics and new criterion for combustion processing", *Nat. Commun.*, vol. 5, no. 1, p. 4908, Dec. 2014, doi: 10.1038/ncomms5908.

[29] S.-W. You and I.-H. Kim, "Solid-state synthesis and thermoelectric properties of Bi-doped Mg_2Si compounds", *Curr. Appl. Phys.*, vol. 11, no. 3, pp. S392–S395, May 2011, doi: 10.1016/j.cap.2011.03.017.

[30] N. Farahi *et al.*, "Sb- and Bi-doped Mg_2Si: location of the dopants, micro- and nanostructures, electronic structures and thermoelectric properties", *Dalton Trans*, vol. 43, no. 40, pp. 14983–14991, Jun. 2014, doi: 10.1039/C4DT01177E.

[31] S. Fiameni *et al.*, "Synthesis and characterization of Bi-doped Mg_2Si thermoelectric materials", *AIP Conf. Proc.*, 2012, vol. 1449, pp. 191–194, doi: 10.1063/1.4731529.